International Journal of Scientific Engineering and Science
Volume 8, Issue 9, pp. 40-51, 2024. ISSN (Online): 2456-7361

Multi-Objective Optimization for Hybrid Microgrid Integration Using a Modified Firefly Algorithm

Edrees Yahya Alhawsawi[1], Darrin Hanna[1], Mohamed A. Zohdy[1], Hao Yan[1]
[1]Department of Electrical and Computer Engineering, Oakland University, Rochester, MI 48309, USA
*Corresponding author: ealhawsawi@oakland.edu

***Abstract*— *This paper presents a multi-objective optimization method utilizing a modified Firefly Algorithm (MFA) to optimize a hybrid grid-connected microgrid that integrates wind and diesel power sources, validated through a case study of such a microgrid. The MFA aims to enhance Net Present Cost (NPC), Levelized Energy Cost (LCOE), reliability, and greenhouse gas (GHG) emissions. The beta parameter in the MFA was dynamically adjusted based on the alpha, theta, and gamma parameters, influencing the attractiveness and movement of fireflies in the optimization process. The MATLAB simulation results demonstrate that the MFA significantly outperforms the original Firefly Algorithm (FA), with an overall improvement of 16%. These findings highlight the MFA's superior performance in enhancing cost-efficiency and reducing environmental impact compared to the original FA. The MFA results were categorized into economic metrics, including NPC, LCOE, and environmental greenhouse gas emissions (GHG) measured as CO_2.*

***Keywords*— *Renewable energy, Microgrid (MG), Multi-objective optimization (MOO), Firefly (FA), Modified Firefly (MFA).*

I. INTRODUCTION

Over the past ten years, there have been significant changes in global civilization, especially in emerging nations. Global energy demand has dramatically increased due to the advancement of digital technologies and the growing population [1]. The primary energy sources are finite fossil fuels, such as coal, natural gas, and oil [2]. Although there is an ample supply of these sources, they are limited in quantity and release greenhouse gases, which hurt the ecosystem. Renewable Energy Sources (RES) contribute to this overarching trend, alongside the development of innovative methods for grid regulation. Consequently, there is an increasing fascination with renewable energy sources, regarded as a more sustainable substitute [3]. RES, such as wind and solar systems, are seeing significant growth and are often considered environmentally beneficial and sustainable due to their economically efficient installation. Furthermore, their sustainability and environmentally benign characteristics make them crucial domestic assets, greatly assisting in reducing dependence on outside power [4]. In contrast to traditional energy sources, renewable energy is characterized by its unpredictability and variability [5]. Meteorological conditions and wind speeds for renewable energy sources can vary significantly depending on the time of day or hour. The presence of this fluctuation provides a degree of uncertainty that is challenging to quantify, which in turn poses difficulties for ensuring the dependability and consistency of the energy system. As a renewable energy source (RES), wind energy is notable for its high effectiveness, reliability, and low maintenance requirements. Moreover, wind power produces significantly lower carbon dioxide (CO_2) emissions and promotes a quieter environment [1]. However, wind energy systems, which are swiftly growing as distributed generation sources, face technical challenges due to their vulnerability to operational failures [6].

Operational management of microgrids is a multi-objective optimization challenge. Traditional optimization methods often fail to effectively balance the trade-offs between conflicting objectives [7]. Therefore, optimization algorithms, such as the Multi-Objective Firefly Algorithm, are essential for providing comprehensive solutions [8]. Ensuring the economic viability of microgrid operations necessitates cost-effective management strategies, highlighting the importance of innovative optimization techniques. High energy reliability in microgrids requires sophisticated energy management systems that can optimize electricity generation, storage, and distribution [9]. Consequently, this involves maximizing the use of renewable energy and ensuring that energy storage systems are used effectively to balance supply and demand. Moreover, reliability is critical to microgrid operations, especially for applications where an uninterrupted power supply is essential [10]. This necessitates maintaining a stable and continuous power supply, managing the variability of renewable energy sources, and ensuring that backup generators and storage systems are ready to compensate for any shortfalls [11].

In the optimization of microgrid systems, ensuring feasibility and practicality are paramount [12]. Several constraints need to be considered to guarantee that the solutions obtained are viable and meet operational requirements. One crucial constraint is ensuring that the total power generated by the system matches the load demand, preventing either under or over-generation [13]. This constraint is typically formulated as an equality constraint, where the sum of power generated by all sources (including renewable and conventional) must equal the total load demand at each time step. Additionally, constraints related to individual components' capacity and operational limits within the microgrid must be enforced. For example, the maximum power output of renewable energy sources such as solar photovoltaic panels and wind turbines, as well as the maximum power output and fuel consumption CHP model, need to be considered [14]. Constraints that are related to the storage capacity and charging/discharging rates of energy storage systems, such as batteries, must be considered [15].

International Journal of Scientific Engineering and Science
Volume 8, Issue 9, pp. 40-51, 2024. ISSN (Online): 2456-7361

TABLE 1. Performance metrics evaluation of Pareto solutions obtained by the modified FA in the four scenarios.

Ref	Campus name	Resources	Method/ optimization	Load Types	Contribution	Results
[2]	Oakland University	Grid, PV, ESS, CHP, and WT	HOMER Pro	Campus load	Advance renewable energy integration within MG systems, plan and design hybrid renewable solutions	NPC of USD 30 M, LCOE of 0.00274 USD/kWh, addressing unmet load, potential for sustainable energy solutions
[16]	-	PV, ESS, and WT		-	Demonstrates the importance of accurate wind speed distribution parameters for optimal Hybrid Renewable Energy System sizing	Errors in the Cost of Energy range from -56.437% to +97.05% depending on the system and parameters used, highlighting the need for accurate parameter setting in energy system modeling.
[17]	-	PV, WT, and DG		Healthcare centers in rural Nigeria	Address inadequate power supply in rural Nigerian healthcare centers with hybrid renewable energy systems.	Optimized configurations in six locations with energy costs ranging from \$0.0588/kWh to \$0.115/kWh; load-following dispatch strategy ensures power availability.
[18]	Najran Secondary Industrial Institute (NSII)	PV, BSS, and Grid		Industrial Institute	Investigates optimal microgrid installation on NSII buildings; integrates architectural design and system administration	Found optimal tilt 20.97° and azimuth 50°; reduces NPC by 54.69% and CO_2 emissions by 92% compared to current grid system
[19]		WT, PV, battery storage, biomass, micro-hydro		Remote areas	Sensitivity analysis	Found PV-WT-MH-CT-BT-DG-BG as the most feasible system with the lowest energy cost, low NPC, and high environmental benefits (81.2% renewable factor)
[20]	-	WT, PV, micro-turbines, diesel/biogas generators, fuel cells, battery storage		Rural villages, business organization, urban residential building	Economic feasibility, different load profiles, performances of the batteries	Li-ion batteries found to be more viable than LA; includes cost, emissions, and performance comparison of battery types and generation sources
[21]	-	WT, PV, hydrogen storage, diesel generator, battery storage, tidal current farm		Proposes a game-based planning method for interconnected microgrids on an island; focuses on data privacy and renewable energy seasonality		Verified effectiveness through case studies; incorporates mixed strategy equilibrium in decision-making
[22]	National University of Sciences and Technology	PV plant, Electric vehicles, Diesel generator	Mix Integer Linear Programming (MILP), Ant Colony Optimization, Linear Programming (LP)	Campus load	Reduction of operational cost, Analysis of distributed generators and optimally scheduled energy storage system (ESS), Comparison of MILP, Ant Colony Optimization, and LP	ESS using MILP minimizes operational costs from \$798.560 to \$756.3850. Economic and environmental benefits discussed
[23]	University Campus in Brazil	PV generation, Battery Energy Storage System (BESS	Simulated Annealing algorithm	Campus energy consumption	Energy management system coordination, Optimal operation of battery system, Reduction in energy consumption costs	Minimize campus energy consumption costs.
[24]	NFC Institute of Engineering and Technology	Photovoltaic system, Energy Storage System, Electric Vehicles	Linear optimization problem, MATLAB simulations	Campus load	Integration of PV system, ESS, and EV in a University campus, Optimal Energy Management System (EMS)	EMS decreases energy consumption cost by nearly 45%, EV as a source reduces energy cost by 45.58%, EV as a load reduces energy cost by 19.33%, Continuous power supply impact analyzed

These constraints ensure that the system operates within safe and efficient limits while meeting the required energy demand. This complexity necessitates innovative optimization techniques. Authors in [1] summarized different microgrid optimization techniques as Table 1 illustrates.

The rest of the paper is as follows: Part 2 Wind energy in Saudi Arabia. Section 3 analyzes Firefly and Modified Firefly algorithms equations. Section 4 mathematical models of various microgrid components. Section 5 Implementation. Section 6 Results and discussion.

II. Wind Energy in Saudi Arabia

Saudi Arabia is increasingly incorporating wind energy into its renewable energy strategy to diversify its energy portfolio

International Journal of Scientific Engineering and Science
Volume 8, Issue 9, pp. 40-51, 2024. ISSN (Online): 2456-7361

and decrease dependence on fossil fuels. The Kingdom's Vision 2030 aims to fulfill 10% of its energy requirements through renewable sources, such as wind and solar power, by the year 2030 [25]. The Kingdom's commitment to wind energy is further evidenced by its collaboration with a consortium led by Japan's Marubeni Corp for 1,100 MW of wind energy, achieving record low prices. These projects include the 600-MW AlGhat and 500-MW Wa'ad Alshamal wind farms, which were announced during the Saudi-Japan Vision 2030 Business Forum. The AlGhat project has set a global record with an electricity cost of USD 15.655 per MWh, while the Wa'ad Alshamal project follows closely with USD 17.018 per MWh. Together, these wind farms are expected to provide power to 257,000 homes annually and contribute significantly to Saudi Arabia's goal of reaching 50% renewable energy by 2030 [26].

Significant research has highlighted the potential and feasibility of wind energy across various regions in Saudi Arabia. For example, a five-year study at Sharma, Al Qurayyat, and Sakaka revealed that Al Qurayyat had the highest mean wind speed and wind power density (WPD), making it an ideal location for wind farm development [27]. Furthermore, a techno-economic feasibility study for a 15 MW wind farm in Qaisumah, Eastern Province, demonstrated the site's capability to generate approximately 23,590 MWh per year, with an estimated energy generation cost of \$0.0487 per kWh [28].

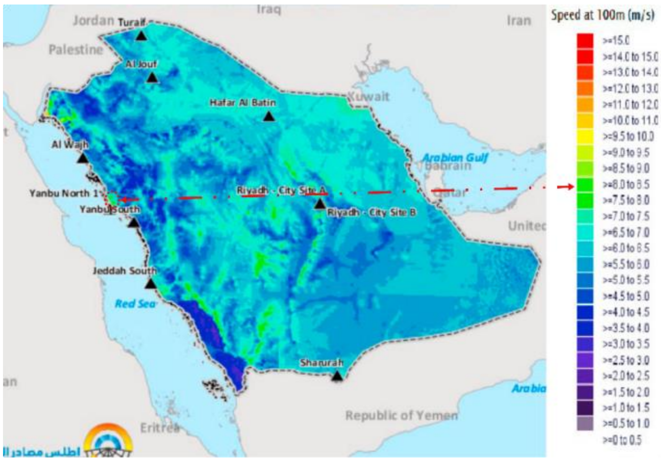

Fig. 1. Wind speed map of Saudi Arabia [33].

In addition, the Dumat Al-Jandal project, the first large-scale wind farm in Saudi Arabia, represents the country's progress in wind energy. Using the System Advisor Model (SAM) software, this 400 MW project was analyzed, revealing a capacity factor ranging from 23.7% to 35.5% depending on hub height, with the lowest levelized cost of energy (LCOE) at 0.323 \$/kWh, demonstrating its economic viability[29]. Coastal areas along the Red Sea, including Al Wajh, have also been identified as favorable locations for wind energy development due to their high wind speeds and suitable conditions for monopile installations [30]. Moreover, particle swarm optimization techniques have been utilized to optimize the cost of energy (COE) for wind farms in Saudi Arabia, revealing that COE is more influenced by rotor size than hub height [31]. Overall, Saudi Arabia's extensive research and strategic policies in harnessing wind energy position the nation as a significant player in the global renewable energy sector [25, 32]. The study will consider an educational building in Yanbu City in the Al Madina Region of Saudi Arabia. According to the Renewable Resource Atlas website, this city has an average wind speed of over 8 m/s, which makes it suitable for installing wind turbines and generating electricity.

III. Firefly Algorithm (FA)

The Firefly Algorithm (FA), developed by Yang, is a metaheuristic algorithm inspired by swarm intelligence [34]. It represents an innovative approach rooted in ecological intelligence, designed to address complex optimization challenges [35, 36]. This search algorithm draws inspiration from firefly social interactions and bioluminescent communication. Two key aspects of FA are the definition of attractiveness and the adjustment of light intensity [37]. This algorithm emulates the social interactions of fireflies as they move through the tropical summer sky. Fireflies use flashing patterns to communicate, search for target, and attract other fireflies, particularly those of the opposite sex. Natural behaviors can be emulated to create metaheuristic algorithms inspired by nature. To streamline the design of a firefly-inspired algorithm, certain characteristics of fireflies' flashing are idealized, resulting in three simplified rules: (1) All fireflies are considered the same sex, ensuring that each firefly can be attracted to any other, regardless of sex. (2) A firefly's brightness is directly correlated with its attraction, and brightness decreases with increasing firefly distance. For any pair of flashing fireflies, the dimmer one will move towards the brighter one. If any brighter fireflies do not surround a firefly, it will move randomly within the search space. (3) The objective function influences or determines A firefly's brightness. The brightness in the optimization problem is very similar to the value of the cost function. Analogously to the fitness function in the PSO algorithm, different types of brightness can also be defined. The FA is updating the formula for every firefly pair; the position of a firefly i moving towards a brighter firefly j is given by [38]:

$$x_i^{(t+1)} = x_i^{(t)} + \beta_0 e^{-\gamma r_{ij}^2}\left(x_j^{(t)} - x_i^{(t)}\right) + \alpha \epsilon_i^{(t)} \qquad (1)$$

Where:

- x_i an x_j are the positions of the Fireflies i and j.
- β_0 : the initial attractiveness.
- γ: the light absorption coefficient.
- r_{ij}: the distance between Fireflies i and j.
- α: the random movement coefficient.
- ε_i: the random vector is drawn from a uniform distribution.

A. *Modified Firefly Algorithm*

The Modified Firefly Algorithm (MFA) is introduced to enhance multi-objective optimization. The MFA procedures are as follows: first, a dynamic attractiveness coefficient is introduced and adapted based on each firefly's multi-objective performance. This coefficient, $\beta_{ij}(t)$, is designed to account for the Pareto dominance relationship between fireflies (i) and (j), ensuring that fireflies move towards more dominant solutions. The distance calculation is also modified to incorporate a weighted sum of normalized distances for each objective. This modification enhances the distance metric to accurately capture the trade-offs among different objectives, ensuring that movement decisions are based on a comprehensive understanding of the solution space. Ultimately, the integration of an adaptive technique for reducing randomness systematically reduces randomness over time. This strategy is specifically designed for multi-objective optimization, balancing the need to explore the search space with the exploitation of advantageous regions, thereby enhancing the algorithm's efficiency in achieving optimal solutions.

B. MFA equations

- Dynamic Multi-Objective Attractiveness:

Dynamic Attractiveness is defined based on Pareto dominance:

$$\beta_{ij}(t) = \beta_0 \left(1 + \frac{n_{dom}(j) - n_{dom}(i)}{n_{total}}\right) e^{-\gamma r_{ij}^2} \quad (2)$$

$\beta_{ij}(t)$: the dynamic attractiveness based on Pareto dominance.
$n_{dom}(j)$: the number of solutions dominated by firefly (j).
$n_{dom}(i)$: the number of solutions dominated by firefly (i).
n_{total}: the total number of fireflies.

r_{ij}: the multi-objective distance calculated using the weighted sum of normalized distances

- Multi-Objective Distance Calculation:

$$r_{ij} = \sqrt{\sum_{k=1}^{M} \omega_k \left(\frac{f_k(x_i) - f_k(x_j)}{f_k^{max} - f_k^{max}}\right)^2} \quad (3)$$

M: the number of objectives
ω_k: the weight assigned to the k-th objective.
f_k^{max} and f_k^{max}: are the maximum and minimum values of k-th objective across all fireflies.

- Adaptive Randomness Reduction

Implement an adaptive randomness reduction mechanism:

$$\alpha(t) = \alpha_0 \exp\left(-\frac{t}{Iter_{max}}\right) \quad (4)$$

α_0: the initial random movement coefficient.
t: the current iteration numbers.
$Iter_{max}$: the maximum number of iterations.

- Update Equation:

$$x_i^{(t+1)} = x_i^{(t)} + \beta_{ij}(t)\left(x_j^{(t)} - x_i^{(t)}\right) + \alpha(t)\epsilon_i^{(t)} \quad (5)$$

$\beta_{ij}(t)$: incorporates multi-objective attractiveness.
$\alpha(t)$: the time-adaptive randomness reduction.

- Pseudo-code:

Algorithm 1: The Proposed MFA

Steps:

1. **Initialize** the positions x_i (for $i = 1,2, \dots, N$) randomly in the solution space:
   - This correctly specifies the initialization of firefly positions.
   - Evaluate the light intensity I_i for each firefly based on the objective functions $f_k(x)$:
     - This is correct, as the objective function values determine light intensity.
2. **While** (termination condition not met):
   - Increment iteration t:
     - This ensures the loop progresses through the specified number of iterations.

For each firefly i from 1 to N:
For each firefly j from 1 to N:
If $I_j > I_i$ (i.e., firefly j is brighter than firefly i):
This correctly checks if firefly j is brighter than firefly j.
Calculate the multi-objective distance r_{ij} between fireflies i and j:
This step is correct; it computes the distance considering all objectives.
Calculate the dynamic attractiveness $\beta_{ij}(t)$
This is correct; it dynamically adjusts attractiveness based on Pareto dominance and the multi-objective distance.

- Move firefly i towards firefly j using the **Improved Update Equation**, which correctly updates the position of firefly i, considering attractiveness and random movement.

End If
End For (j)
Evaluate the new light intensity $I_i^{(t+1)}$ for firefly i:
This correctly updates the light intensity based on the new position
End For (i)
Reduce the randomness $\alpha(t)$ which is correctly models the decrease in randomness over time.
Sort the fireflies based on their updated light intensity.
Sorting is crucial to determining the best global positions and helps in guiding the search process.
End While

Output:
The best firefly positions (x) **and elapsed time**: This provides the final solution set and the time taken to reach it.

IV. MATHEMATICAL MODELS OF MICROGRID COMPONENTS

This section presents the mathematical models for the microgrid's primary components, including generators, energy storage systems, and load demands.

A. Generator Models

Microgrid generators include renewable sources such as Wind Turbines (WT), and conventional power sources such as Diesel Generator (DG). Each type of generator is modelled to reflect its operational characteristics and constraints [12].

1. Wind Turbine Model:

The Wind Turbine (WT) transforms kinetic energy from the wind into electrical energy. Among various renewable energy sources, wind energy boasts a high conversion efficiency. Nevertheless, the significant initial investment and dependence on weather conditions pose challenges to fully harnessing wind energy. Moreover, Wind speed and the electricity generated by WT have a nonlinear relationship. The power output of a wind turbine is a function of the wind speed $V(t)$ [14]. The wind turbine output power output is modelled as:

$$WT_P(t) = \begin{cases} WT_N, & V_{ci} \le V(t) \le V_r \\ WT_N \times n_w \times \left(\frac{V(t)^3 - V_{ci}^3}{V_r^3 - V_{ci}^3}\right) \times WT_{pr}, & V_r < V(t) \le V_{co} \\ 0, & V(t) < V_{ci} \text{ or } V(t) > V_{co} \end{cases} \quad (6)$$

$WT_P(t)$: Total power output from the wind turbine
WT_N: Number of wind turbines
WT_{Pr}: Rated power output of a single wind turbine
n_w: Efficiency factor or other modifier based on the wind turbine's performance.
$V(t)$: Wind speed at time t
V_{ci}: Cut-in wind speed, or the minimum wind speed at which the turbine starts.
V_r: Rated wind speed, or the wind speed at which the turbine generates its rated power.
V_{CO}: Cut-out wind speed, or the maximum wind speed at which the turbine is designed to operate.

2. Diesel Generator Model:

Enhancing the operational stability of the hybrid microgrid system by ensuring the load demand is met when renewable energy sources (RESs) are insufficient, the standalone diesel generator connected to the AC bus serves as a backup source. When the output power is low, the capacity of the generator is still low [39]. The diesel generator's fuel consumption $F_{DG}(t)$ and power output $P_{DG}(t)$ are modelled as [15]:

$$F_{DG}(t) = \mathrm{a} + \mathrm{b} \cdot P_{DG}(t) \quad (7)$$

Where:
a is the fuel curve slope coefficient, and b is the fuel intercept coefficient are fuel consumption coefficients (L/kWh), values are considered to be 0.246 and 0.08415 [40].

3. Load Demand Model:

The load demand $P_{load}(t)$ represents the power consumption at time t [41]. It can be modelled based on historical consumption data. The load demand equation is expressed as:

$$P_{load}(t) = P_{base}(t) + P_{variable}(t) \quad (8)$$

Where:

- $P_{base}(t)$ is the base load demand,
- $P_{variable}(t)$ is the variable load demand, which may depend on factors such as weather conditions and occupancy rates.

Equation 8 represents the electricity demand at any time, dividing it into base load (constant consumption for essential functions) and variable load (fluctuating demand due to factors like weather and occupancy). The base load remains constant for essential functions, while the variable load changes with weather conditions, as heating and cooling systems consume more power during extreme temperatures and occupancy. rates. Ensuring sufficient power is available to meet the demand while minimizing reliance on the utility grid or expensive generators helps optimize microgrid operation.

4. Microgrid Power Balance:

To ensure stable operation [42], the microgrid must maintain a power balance at all times. The power balance equation is expressed as:

$$WT_P + P_{DG}(t) + P_{Grid}(t) = P_{load}(t) \quad (9)$$

Where:
WT_P: the power generated by the wind turbine.
$P_{DG}(t)$: the power generated by the diesel generator.
$P_{Grid}(t)$: the grid power.
$P_{load}(t)$: the load demand.

B. Objective functions

Multi-objective optimization aims to optimize two or more objectives simultaneously and balance them to achieve the best possible trade-off between conflicting goals. LCOE, CO_2 emissions, and reliability are used in multi-objective optimization to find a Pareto front. These objectives often conflict, requiring trade-offs to identify optimal solutions. The Pareto front will show the best trade-offs were improving one objective may worsen another.

C. Cost Parameters

1. NET PRESENT COST (NPC):

The Net Present Cost (NPC) encompasses the fuel costs (FC), replacement costs (Replacement), operation and maintenance (O&M) expenses, and the initial investment associated with the DG. Although RES usually have low operating and maintenance costs because they don't require fuel, their initial construction costs can be substantial. The NPC is calculated as follows [43, 44]:

$$\sum_{t=1}^{t} f_{dr}\,(D_{cap} + D_{rep} + D_{O\&M} + D_{fule}) \quad (10)$$

Where: f_{dr}: discount rate, D_{cap}: capital cost, D_{rep}: replacement cost, $D_{O\&M}$: Operation and maintenance, D_{fule}: fuel cost.

$$f_{dr} = \frac{1}{(1+f)^n} \quad (11)$$

$$f = \frac{f^{\iota} - i}{f + i} \quad (12)$$

Where: f^{ι}: interest rate and I represent the inflation rate.

$$D_{ann} = \mathrm{DRF(f, n)} \times \mathrm{NPC} \quad (13)$$

D_{ann}: Annual cost

$$\mathrm{DRF(f, n)} = \frac{f(1+f)^n}{(1+f)^n - 1} \quad (14)$$

In the proposed system, the primary energy supply comes from the utility grid and wind turbine generators, with diesel generators serving as a backup. Figure 1 illustrates the flowchart of the recommended energy management strategy. This paper introduces four scenarios aimed at addressing the multi-objective problem.

2. OBJECTIVE 1: (f_1) LEVELIZED COST OF ENERGY (LCOE):

Levelized Cost of Energy (LCOE) accounts for the power outputs from the grid, wind turbine, and diesel generator, along with their respective cost coefficients, to determine the LCOE over a specified time horizon and calculated as follows [45]:

$$f2(x) = \frac{\sum_{t=1}^{T}(P_{Grid}(t)\cdot C_{Grid}+P_{WT}(t)\cdot C_{WT}+P_{DG}(t)\cdot C_{DG}}{\sum_{t=1}^{T} P_{total}} \quad (15)$$

- $P_{Grid}(t), P_{WT}(t), P_{DG}(t)$: are the power outputs from the grid, wind turbine, and diesel generator at a given time, respectively.
- C_{Grid}, C_{WT}, C_{DG}: are the cost coefficients for each power source.

3. OBJECTIVE 2: (f_2) GREEN HOUSE GAS MINIMIZATION:

This study estimated greenhouse gas (GHG) emissions from using the grid, wind turbines, and diesel generators. Emissions were calculated for a baseline scenario using the grid and wind turbines to meet the load. This was then compared with a proposed system incorporating renewable and conventional energy sources (grid, wind turbines, and diesel) to determine the net savings in GHG emissions. Saudi Arabia's grid emission factor is approximately 0.559 kg CO_2/kWh [46]. Wind energy generates around 0.011 kg CO_2/kWh [47]. Diesel generators, with emissions varying based on characteristics and fuel, typically emit 2.4–2.8 kg CO_2 per liter of diesel consumed. [48]. Specifically, for a diesel generator rated at 500 kW, the emission factor considered was 1.27 kg CO_2/kWh, equivalent to 3.15 kg CO_2/kWh [49], and 3.50 kg CO_2/kWh. Carbon footprints can also be expressed in kg carbon and converted to kg CO_2 by multiplying by 0.27 [50]. The overall GHG emission of the microgrid is expressed as:

$$GHG = E_{Grid} + E_{WT} + E_{DG} \quad (16)$$

Where:

$E_{Grid}, E_{WT}\ E_{DG}$: are the emission coefficients for each power source.

4. OBJECTIVE 3: RELIABILITY (f_3):

The reliability of the microgrid system is assessed using the Loss of Power Supply Probability (LPSP). LPSP is a statistical measure that indicates the probability of the power supply failing to meet the load demand due to technical issues or insufficient energy production. The LPSP value ranges from 0 to 1 and is calculated using the following equation [51, 52]:

$$LPSP\ \% = \frac{\sum_{t=1}^{T}(P_{demand}(t)-P_{grid}(t)+P_{WT}(t)+P_{DG}(t))}{\sum_{t=1}^{T} P_{demand}(t)} \quad (17)$$

Where:

$P_{demand}(t)$: represents the load demand at time (t).
$P_{grid}(t)$: Power supplied by the utility grid at time (t).
$P_{WT}(t)$: power generated by wind turbines at time (t).
$P_{DG}(t)$: power generated by diesel generators at time (t).

The LPSP is evaluated under the condition that the total load demand exceeds the combined energy generation from all sources

$$P_{demand}(t) > P_{generate}(t) \quad (18)$$

Where: $P_{generate}(t)$ represents the total power generated at time (t) from all available power sources.

D. Constraints

The objectives functions are restricted by the constraints set forth by the specified limitations provided.

1. LIMITS OF DECISION VARIABLES:

Boundaries of decision variables are a critical aspect to consider in the realm of decision-making.

$$N_y^{min} \le N_y \le N_y^{max}, y \in \{Grid, WT, DG\} \quad (19)$$

Where: N_y represents the number of components y.

The determination of upper and lower limits for decision variables is inherently problem-specific, shaped by factors like the search space complexity and the number of variables. Optimization algorithms often establish these boundaries through iterative refinement and trial and error.

2. ENERGY BALANCE CONSTRAINT:

The energy balance constraint is the fundamental equation governing the entire optimization problem. It ensures that at any given time t, the total power generated and stored must meet the demand for power plus any losses in the system [53]. The following equation can express this:

$$E_{grid}(t) + E_{WT}(t) + E_{DG}(t) \ge E_{load}(t) \quad (20)$$

Where: $E_{grid}(t)$: Energy from the utility grid at time (t).
$E_{WT}(t)$: Energy generated by wind turbines at time (t).
$E_{DG}(t)$: Energy generated by diesel generator at time (t).

Essentially, this equation states that the sum of all energy generation sources must equal the sum of the load demand. This constraint ensures that the power system remains stable and avoids situations such as blackouts caused by insufficient power generation or overloading of the grid.

3. GENERATOR OPERATIONAL LIMITS RAINT:

The energy balance constraint ensures the overall system remains stable, but each generator also has its own operational limits that must be respected [54]. These limits are crucial for guaranteeing the safe and efficient operation of the generators and extending their lifespan. The following equations represent these constraints:

$$0 \le E_{WT}(t) \le E_{WT}, max \quad (20)$$
$$0 \le E_{DG}(t) \le E_{DG} max \quad (21)$$

Where: max represents the maximum energy output capacity of that generator type. These constraints essentially define each generator's operating range.

4. PROPOSED FRAMEWORK:

Microgrids encounter the intricate challenge of optimizing their operations by balancing three critical objectives: cost, emission reduction, and reliability. An effective Energy Management Operations Strategy (EMOS) tackles this "trilemma" by testing various scenarios, prioritizing one objective while ensuring the others are adequately balanced. This strategy is especially crucial in systems where data includes detailed information on the energy costs of different power sources.

Volume 8, Issue 9, pp. 40-51, 2024.

International Journal of Scientific Engineering and Science
ISSN (Online): 2456-7361

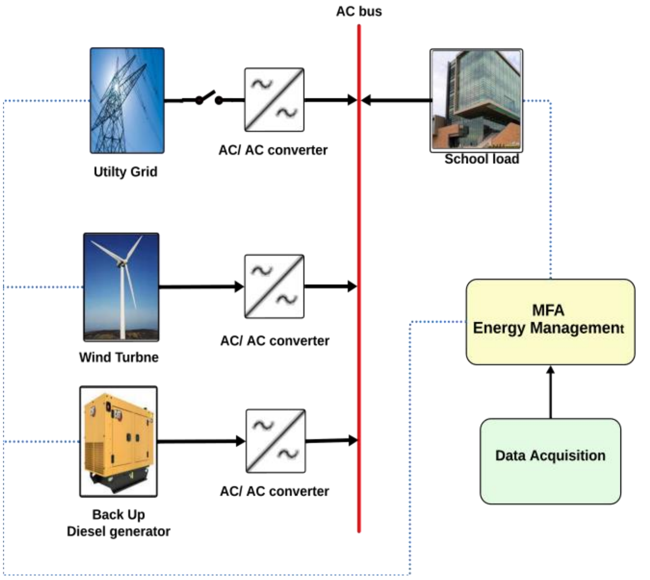

Fig. 2. Proposed Framework for Microgrid Energy Management

The framework depicted in the figure employs data acquisition to monitor load demand, meteorological conditions, and the rated power of all energy sources to evaluate the current operating state. This information is then processed by the Modified Firefly Algorithm (MFA), which uses predefined decision variables such as the Grid, Wind Turbine (WT), and Diesel Generator (DG), as shown in Figure 2.

MFA functions as the central controller, regulating the distribution of electricity between various power sources and the load demand. It interfaces with the Main Service Panel, which is responsible for distributing power to the load and the grid. Data acquisition tools are employed to gather information from the utility grid, weather forecasts, energy prices, and the operational status of renewable energy sources [55-58]. Wind turbines contribute to renewable energy production, while the diesel generator serves as a backup power source. Their outputs are managed dynamically to optimize efficiency and reliability. This proposed energy management framework integrates MFA's technologies and optimization algorithms to achieve a balance between cost minimization, emission reduction, and reliability enhancement. This comprehensive solution is designed to meet the unique energy requirements of a university campus, promoting sustainable energy management and operational excellence.

V. IMPLEMENTATION

The Modified Firefly Algorithm (MFA) was implemented in MATLAB 2024 a. The algorithm defines objective functions such as levelized cost of Energy (LCOE), greenhouse Gas (GHG), and reliability.

A. Data visualization

1. WIND SPEED:

Leveraging wind speed data in Saudi Arabia, a viable and sustainable solution for generating wind power has been identified for Yanbu City, where the average wind speed reaches 8 m/s. [33]. The graph displays the wind speed data for one year. The x-axis represents time, and the y-axis displays wind speed in meters per second (m/s). Figure 3 highlights clear seasonal differences, with higher wind speeds occurring in the first half of the year, especially around February to May and from September to December, reaching peaks of approximately 12–13 m/s. The average wind speed through the year ranges from 6 to 8 m/s. The data shows a consistent annual pattern of fluctuating wind speeds, characterized by distinct monthly peaks and valleys.

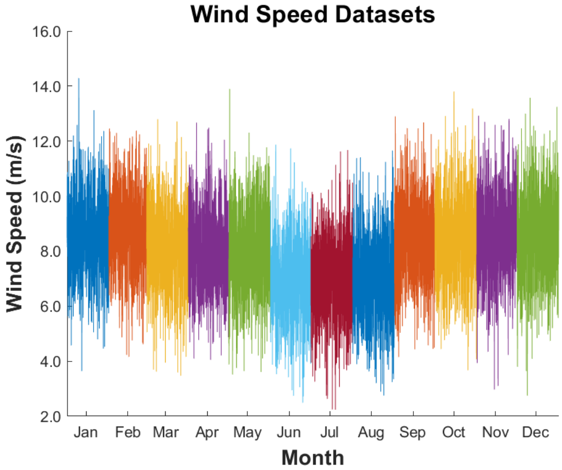

Fig. 3. Annual wind Speed of the site.

This visualization is crucial for optimizing wind energy generation strategies in several ways: Analyzing wind patterns can help integrate wind turbines more effectively, thereby reducing dependence on diesel generators. Operating turbines primarily during periods of high wind, such as February, minimizes the need for backup power sources and results in significant cost savings. Coordinating wind turbine operations with high wind periods, particularly from November to March, optimizes energy capture and efficiency.

2. LOAD DEMAND:

Figure 4 illustrates variations in power use by looking at the load demand over a whole year. This evaluation uses a dataset that details the hourly load demand in kilowatts (KW) throughout the year. Each month's load demand is depicted in a different color, allowing for a clear visual comparison of the power consumption patterns over time. Load demand experiences notable peaks and troughs all year long. For instance, peak load demand can be observed reaching up to approximately 30 KW, particularly during the mid-year months. This indicates periods of high energy consumption, which might be due to increased activity or specific seasonal requirements.

This detailed visualization helps to understand the school building's dynamic energy consumption patterns, identifying peak demand periods and highlighting seasonal variations. Such insights are crucial for optimizing energy management strategies, improving resource allocation, and potentially implementing demand response measures to enhance the facility's power usage efficiency and sustainability.

Volume 8, Issue 9, pp. 40-51, 2024.

International Journal of Scientific Engineering and Science
ISSN (Online): 2456-7361

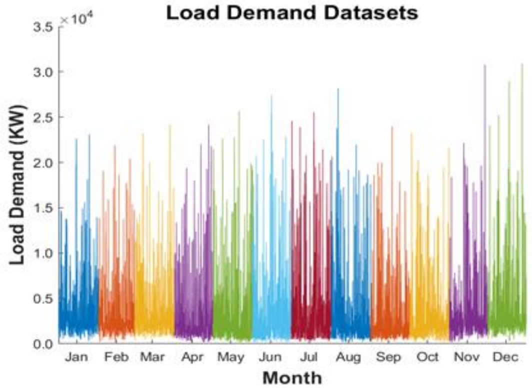

Fig. 4. Lload profile.

B. *Specifications of Microgrid Components*

Table 2 Presents an overview of the technical and financial criteria selected for the components of the microgrid system. [59-62].

TABLE 2. Technical and financial criteria of microgrid components.

Component	Parameter	Value	Unit
WT	Model	Kingspan Renewables	
	Rated power	6	KW
	Cut-in wind speed	3.5	m/s
	Number of blades	3	-
	Lifetime	20+	Year
	Capital Cost	1300	($/kW)
	Replacement Cost	1300	($/kW)
	Maintenance Cost	56	($/kW)
DG	Rated power	1	KW
	Lifetime	50,000	Hours
	Capital Cost	1000	($/kW)
	Replacement Cost	1000	($/kW)
	Diesel Fuel	0.33	($/L)
	replacement and maintenance Cost	1000	($/kW)

VI. Results and Discussion

Four scenarios of power source configurations were evaluated using both the Original and Modified Firefly Algorithms (MFA) It has been observed that the MFA consistently outperformed the Original FA when it came to the reduction of the Net Present Cost (NPC) and the improvement of the Levelized Cost of Energy (LCOE) while ensuring or improving reliability in all scenarios (Figures 5-8).

A. *Scenario 1: Grid, **6** KW wind power and 1KW of DG*

In Scenario 1 (Figure 5 a and b), integrating a capacity of 6 KW wind turbine with a 1 KW diesel generator, the MFA reduced NPC significantly compared to the Original FA, demonstrating its efficiency in mixed energy systems.

B. *Scenario 2: Grid, **6** KW wind power*

Scenario 2 (Figure 6 a and b), using a grid and a capacity of 6 KW wind turbine, showed that MFA lowered costs and improved environmental metrics more effectively than the Original FA.

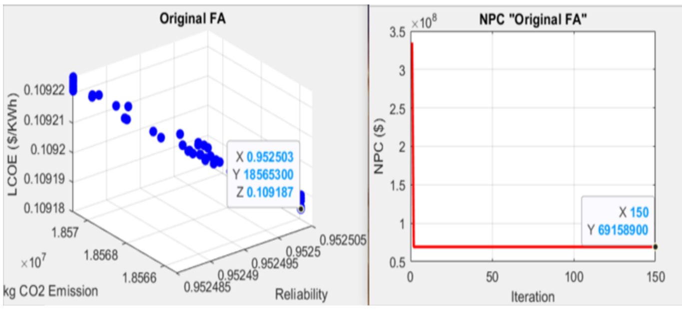

Fig. 5. a Optimization results for MFA-Scenario 1, where the lift figure represents the tradeoff between LCOE, CO_2 emissions and Reliability and right figure represents NPC.

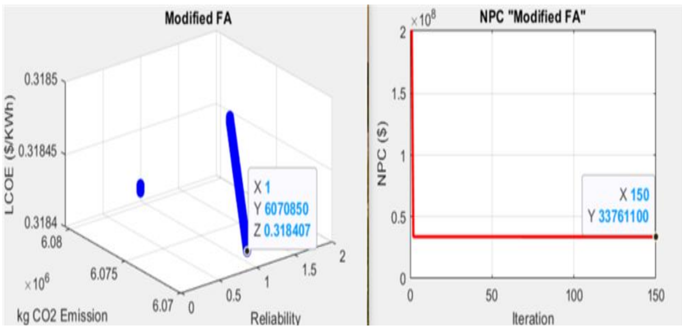

Fig. 5. b Optimization results for MFA-Scenario 1, where the lift figure represents the tradeoff between LCOE, CO_2 emissions and Reliability and right figure represents NPC

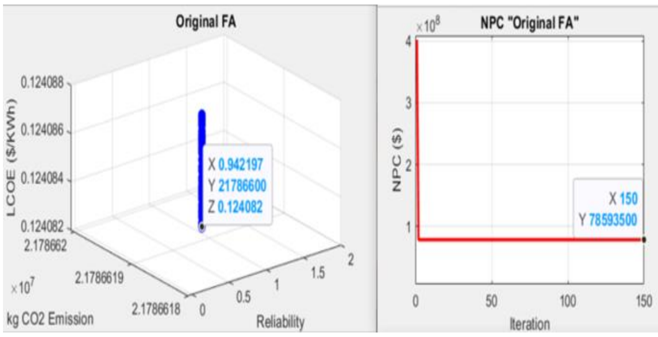

Fig. 6. a Optimization results for FA-Scenario 2, where the lift figure represents the tradeoff between LCOE, CO_2 emissions and Reliability and right figure represents NPC.

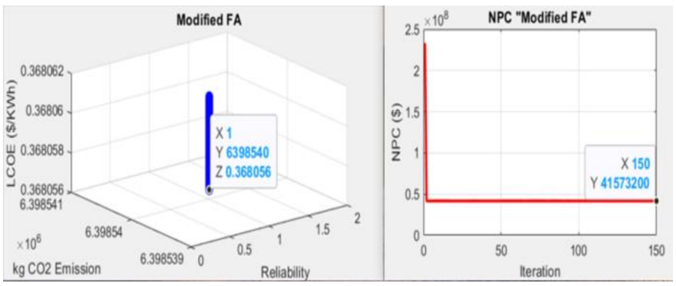

Fig. 6. Optimization results for MFA-Scenario 2, where the lift figure represents the tradeoff between LCOE, CO_2 emissions and Reliability and right figure represents NPC.

C. *Scenario 3: Grid, 18KW wind power and 1KW, of DG*

For Scenario 3 (Figure 7 a and b), which included a capacity of 18 KW wind turbines and a 1 KW diesel generator, the MFA continued to show better results than the Original FA.

International Journal of Scientific Engineering and Science
Volume 8, Issue 9, pp. 40-51, 2024.
ISSN (Online): 2456-7361

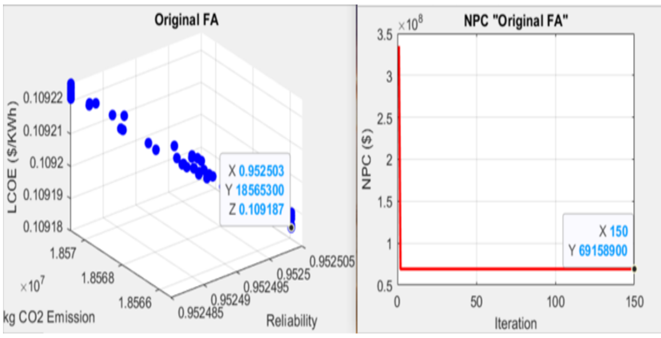

Fig. 7. a Optimization results for FA-Scenario 2, where the lift figure represents the tradeoff between LCOE, CO_2 emissions and Reliability and right figure represents NPC.

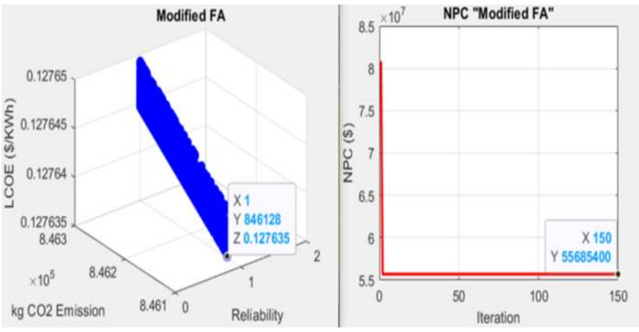

Fig. 7. b Optimization results for FA-Scenario 2, where the lift figure represents the tradeoff between LCOE, CO_2 emissions and Reliability and right figure represents NPC.

D. Scenario 4: Grid, 18kW wind power

In Scenario 4 (Figure 8 a and b), pairing the grid with an 18 KW wind turbine, the MFA delivered the most substantial cost reduction, showcasing its superior performance in systems relying solely on renewable energy.

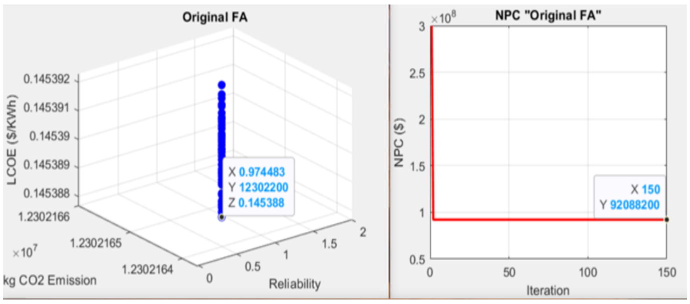

Fig. 8. a Optimization results for FA-Scenario 2, where the lift figure represents the tradeoff between LCOE, CO_2 emissions and Reliability and right figure represents NPC.

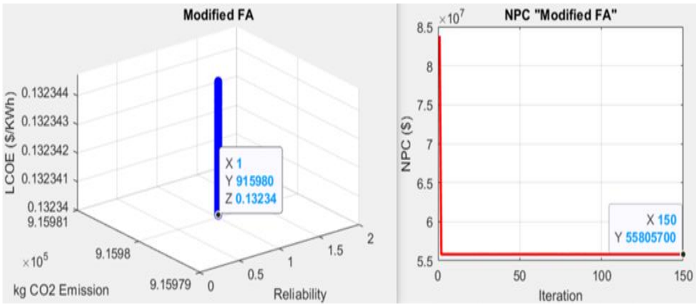

Fig. 8. b Optimization results for FA-Scenario 2, where the lift figure represents the tradeoff between LCOE, CO_2 emissions and Reliability and right figure represents NPC.

Overall, the MFA demonstrated superior performance across all scenarios by effectively reducing costs and enhancing environmental outcomes, outperforming the Original FA in key multi-objective metrics: NPC, LCOE, CO_2 Emission, and Reliability, as illustrated in Table 3.

TABLE 3. Cost and environmental results of optimum energy sources obtained with FA and MFA

Scenario	Power source	Multi-Objectives							
		NPC ($)		LCOE ($/KWh)		CO_2 Emission (Kg)		Reliability	
		FA	MFA	FA	MFA	FA	MFA	FA	MFA
1	Grid, 6KW wind and 1KW DG	69158900	33761100	0.11	0.3	18565300	3070850	0.95	1
2	Grid and 6KW wind	78593500	41573200	0.12	0.36	21786600	6398540	0.94	1
3	Grid, 18 KW wind and 1KW DG	85069700	55685400	0.13	0.12	10078000	8461208	0.97	1
4	Grid and 18KW wind	92088200	55805700	0.14	0.13	12302200	9159180	0.97	1

In the multi-objective optimization of the hybrid energy system, the Modified Firefly Algorithm (MFA) demonstrated considerable improvements over the traditional Firefly Algorithm (FA) across various performance aspects, including Net Present Cost (NPC), Levelized Cost of Energy (LCOE), CO_2 emissions, and system reliability. Since the optimization process simultaneously considers multiple objectives, MFA showed a trade-off where some objectives improved significantly while others worsened. For instance, MFA consistently reduced NPC across all scenarios, achieving reductions between 34.5% and 51.2%, indicating a more cost-efficient energy solution. However, this cost efficiency came with an increased LCOE in some scenarios, with MFA showing some increase in scenarios 1 and 2, respectively. Despite the higher LCOE, MFA significantly reduced CO_2 emissions by 16% to 83.5%, highlighting its effectiveness in minimizing environmental impact. Furthermore, MFA consistently improved system reliability, achieving 100% in all scenarios, compared to FA's reliability range of 94% to 97%. Overall, the MFA provides a more balanced optimization solution, effectively reducing costs and emissions while enhancing reliability, resulting in an overall improvement of approximately 16 % compared to the conventional FA.

E. Performance evaluation of MFA

The performance metrics evaluation of Pareto solutions obtained from the Modified Firefly Algorithm (MFA) indicates a diverse set of optimal solutions across scenarios as in Table 4. Statistical analysis of the Pareto front reveals a range of values for each metric, showcasing variability in the trade-offs achieved. The metrics, including minimum, maximum, range, standard deviation, and mean, illustrate the algorithm's capability to explore and balance different performance aspects effectively. This evaluation underscores the MFA's proficiency in providing a broad spectrum of solutions, reflecting its robustness in addressing multiple objectives simultaneously.

TABLE 4. Performance metrics evaluation of Pareto solutions obtained by the modified FA in the four scenarios.

Scenario	metrics	Min.	Max.	range	STD.	Mean
Scenario 1	LCOE	0.0534	0.3184	0.2650	0.0261	0.0552
	Reliability	0.9850	1	0.0150	0.0012	0.9851
	CO2 Emission	1.3065	6.07009	4.76	0.389	1.34
Scenario 2 No DG	LCOE	0.0656	0.368	0.3024	0.0242	0.0677
	Reliability	0.9828	1	0.0172	0.0014	0.9829
	CO2 Emission	0.96	6.3985	5.4369	0.4439	0.99
Scenario 3	LCOE	0.0879	0.1276	0.0397	0.0032	0.0882
	Reliability	0.997	1	0.0023	0.0002	0.9978
	CO2 Emission	1.319	8.4614	7.1415	0.5831	1.3681
Scenario 4	LCOE	0.08881	0.1323	0.0442	0.0036	0.0884
	Reliability	0.9975	1	0.0025	0.002	0.9975
	CO2 Emission	1.2073	9.159	7.9525	0.6493	1.2610

VII. Conclusion

The Modified Firefly Algorithm (MFA) demonstrated a clear advantage over the traditional Firefly Algorithm (FA) in optimizing hybrid energy systems by effectively balancing multiple objectives such as cost efficiency, environmental impact, and system reliability. It demonstrates MFA's ability to provide cost-effective solutions in all scenarios by consistently reducing Net Present Cost (NPC) by 34.5% to 51.2%. Considering this trade-off, future implementations must consider this cost reduction along with an increase in the levelized cost of energy (LCOE). Future implementations need to consider this trade-off. Despite this, the algorithm's reduction in CO_2 emissions by 16% to 83.5% reinforces its potential in contributing to more environmentally sustainable energy systems. The MFA's ability to achieve 100% system reliability across all scenarios, compared to the FA's reliability range of 94% to 97%, further underscores its effectiveness in ensuring stable and dependable energy systems. Moreover, the comprehensive performance evaluation of Pareto-optimal solutions illustrates the MFA's versatility and robustness in addressing diverse optimization goals simultaneously. Overall, the MFA presented a powerful tool for hybrid energy system optimization, achieving substantial improvements in cost reduction, environmental impact, and reliability. Future research should explore the MFA's application in more complex systems, refining its ability to balance trade-offs and optimize performance under varying conditions. This would further enhance its potential as a key algorithm for advancing sustainable energy solutions.

References

[1] E.Y. Alhawsawi, K. Salhein, and M.A. Zohdy, "A comprehensive review of existing and pending university campus microgrids," Energies, vol. 17, no. 10, pp. 2425, 2024.
[2] E.Y. Alhawsawi, H.M.D. Habbi, M. Hawsawi, and M.A. Zohdy, "Optimal design and operation of hybrid renewable energy systems for Oakland university," Energies, vol. 16, no. 15, pp. 5830, 2023.
[3] M. Mehrpooya and M.M.M. Sharifzadeh, "A novel integration of oxy-fuel cycle, high temperature solar cycle and LNG cold recovery–energy and exergy analysis," Applied Thermal Engineering, vol. 114, pp. 1090–1104, 2017.
[4] D. Saheb Koussa and M. Koussa, "GHGs (greenhouse gases) emission and economic analysis of a GCRES (grid-connected renewable energy system) in the arid region, Algeria," Energy, vol. 102, pp. 216–230, 2016.
[5] H. Yang, W. Zhou, L. Lu, and Z. Fang, "Optimal sizing method for stand-alone hybrid solar–wind system with LPSP technology by using genetic algorithm," Solar Energy, vol. 82, no. 4, pp. 354–367, 2008.
[6] O. Morfín, D. Delgado, A. Campos, M. Murillo, J.I. Hernández, and P. Esquivel, "Fault-tolerant controller applied to a wind system using a doubly fed induction generator," Wind, vol. 4, no. 2, pp. 90–110, 2024.
[7] M.A. Mquqwana and S. Krishnamurthy, "Particle swarm optimization for an optimal hybrid renewable energy microgrid system under uncertainty," Energies, vol. 17, no. 2, pp. 422, 2024.
[8] G. Chen, X. Yi, Z. Zhang, and H. Wang, "Applications of multi-objective dimension-based firefly algorithm to optimize the power losses, emission, and cost in power systems," Applied Soft Computing, vol. 68, pp. 322–342, 2018.
[9] B. Tan and H. Chen, "Stochastic multi-objective optimized dispatch of combined cooling, heating, and power microgrids based on hybrid evolutionary optimization algorithm," IEEE Access, vol. 7, pp. 176218–176232, 2019.
[10] X. Zhang, Z. Wang, and Z. Lu, "Multi-objective load dispatch for microgrid with electric vehicles using modified gravitational search and particle swarm optimization algorithm," Applied Energy, vol. 306, pp. 118018, 2022.
[11] V. Indragandhi, R. Logesh, V. Subramaniyaswamy, V. Vijayakumar, P. Siarry, and L. Uden, "Multi-objective optimization and energy management in renewable based AC/DC microgrid," Computers & Electrical Engineering, vol. 70, pp. 179–198, 2018.
[12] M. Parvin, H. Yousefi, and Y. Noorollahi, "Techno-economic optimization of a renewable micro grid using multi-objective particle swarm optimization algorithm," Energy Conversion and Management, vol. 277, pp. 116639, 2023.
[13] C.A. Nallolla, P. V., D. Chittathuru, and S. Padmanaban, "Multi-objective optimization algorithms for a hybrid AC/DC microgrid using RES: A comprehensive review," Electronics, vol. 12, no. 4, pp. 1062, 2023.
[14] T. Babawurun, D.R.E. Ewim, T.O. Scott, and C. Neye-Akogo, "A comprehensive review of wind turbine modeling for addressing energy challenges in Nigeria and South Africa in the 4IR context," The Journal of Engineering and Exact Sciences, vol. 9, no. 2, pp. 15479–01e, 2023.
[15] X. Dong, J. Huang, N. Luo, W. Hu, and Z. Lei, "Design and implementation of digital twin diesel generator systems," Energies, vol. 16, no. 18, pp. 6422, 2023.
[16] C. Altin, "Investigation of the effects of synthetic wind speed parameters and wind speed distribution on system size and cost in hybrid renewable energy system design," Renewable and Sustainable Energy Reviews, vol. 197, pp. 114420, 2024.
[17] L. Olatomiwa, O.M. Longe, T.A. Abd'Azeez, J.G. Ambafi, K.E. Jack, and A.A. Sadiq, "Optimal planning and deployment of hybrid renewable energy to rural healthcare facilities in Nigeria," Energies, vol. 16, no. 21, pp. 7259, 2023.
[18] M. Abusaq and M.A. Zohdy, "Optimizing renewable energy integration through innovative hybrid microgrid design: A case study of Najran Secondary Industrial Institute in Saudi Arabia," Clean Technologies, vol. 6, no. 2, pp. 397–417, 2024.
[19] Y. Sawle, S. Jain, S. Babu, A.R. Nair, and B. Khan, "Prefeasibility economic and sensitivity assessment of hybrid renewable energy system," IEEE Access, vol. 9, pp. 28260–28271, 2021.
[20] S. Dhundhara, Y.P. Verma, and A. Williams, "Techno-economic analysis of the lithium-ion and lead-acid battery in microgrid systems," Energy Conversion and Management, vol. 177, pp. 122–142, 2018.
[21] H. Li, Z. Ren, A. Trivedi, P.P. Verma, D. Srinivasan, and W. Li, "A noncooperative game-based approach for microgrid planning considering existing interconnected and clustered microgrids on an island," IEEE Transactions on Sustainable Energy, vol. 13, no. 4, pp. 2064–2078, 2022.
[22] A. Ulasyar, H.S. Zad, A. Khattak, and K. Imran, "Optimal day-ahead scheduling for campus microgrid by using MILP approach," Pakistan Journal of Engineering and Technology, vol. 4, no. 2, pp. 21–27, 2021.
[23] J. Angelim and C. Affonso, "Energy management on university campus with photovoltaic generation and BESS using simulated annealing," in Proceedings of the 2018 IEEE Texas Power and Energy Conference (TPEC), pp. 2018.
[24] T. Nasir, S. Raza, M. Abrar, H.A. Muqeet, H. Jamil, F. Qayyum, O. Cheikhrouhou, F. Alassery, and H. Hamam, "Optimal scheduling of

campus microgrid considering the electric vehicle integration in smart grid," Sensors, vol. 21, no. 21, pp. 7133, 2021.
[25] S.F. Al-Gahtani, "Saudi Arabia's journey toward a renewable future," Energies, vol. 17, no. 11, pp. 2444, 2024.
[26] A. Ivanova, "Saudi Arabia signs 1,100 MW of PPAs at 'record low' price for wind," May 22, 2024 [cited July 25, 2024]. Available from: https://renewablesnow.com/news/saudi-arabia-signs-1100-mw-of-ppas-at-record-low-price-for-wind-858548/#:~:text=The%20levelised%20cost%20of%20electricity,al%2DSaud%20said%20on%20Tuesday.
[27] A.H. Alanazi and F.A. Almutlaq, "Assessment of wind energy potential at three prime locations in Saudi Arabia: Analysis of Sharma, Qurayyat and Sakaka Sites," American Journal of Natural Sciences, vol. 5, no. 2, pp. 30–48, 2024.
[28] S. Shaahid, L.M. Alhems, and M. Rahman, "Techno-economic assessment of development of wind farms at a potential location in eastern region of Saudi Arabia—A step towards alternative energy for sustainable future," in Proceedings of the 2024 8th International Conference on Green Energy and Applications (ICGEA), 2024, IEEE.
[29] K. Almutairi and R. Alahmadi, "The feasibility of the first utility-scale wind farm in Saudi Arabia (The 400 MW Dumat Al-Jandal Project)," Journal of Clean Energy Technologies, vol. 10, no. 1, pp. 1–10, 2022.
[30] M.T. Naqash, M.H. Aburamadan, O. Harireche, A. AlKassem, and Q.U. Farooq, "The potential of wind energy and design implications on wind farms in Saudi Arabia," International Journal of Renewable Energy Development, vol. 10, no. 4, pp. 839, 2021.
[31] H. Marouani, Y. Fouad, and H. Mrad, "A techno-economic assessment and optimization of Dumat Al-Jandal wind farm in Kingdom of Saudi Arabia," Energy Science & Engineering, vol. 11, no. 12, pp. 4398–4407, 2023.
[32] F.E.M. Suliman, "Solar-and wind-energy utilization in the Kingdom of Saudi Arabia: A comprehensive review," Energies, vol. 17, no. 8, pp. 1894, 2024.
[33] H. Allhibi, H. Chowdhury, M. Zaid, B. Loganathan, and F. Alam, "Prospect of wind energy utilization in Saudi Arabia: A review," Energy Procedia, vol. 160, pp. 746–751, 2019.
[34] X.-S. Yang, Nature-Inspired Metaheuristic Algorithms, Luniver Press, 2010.
[35] G.G. Wang, L. Guo, H. Duan, and H. Wang, "A new improved firefly algorithm for global numerical optimization," Journal of Computational and Theoretical Nanoscience, vol. 11, no. 2, pp. 477–485, 2014.
[36] N.J. Cheung, X.-M. Ding, and H.-B. Shen, "Adaptive firefly algorithm: parameter analysis and its application," PLoS One, vol. 9, no. 11, pp. e112634, 2014.
[37] D.M. Hanna and M.F. Lohrer, "Emission source localization using the firefly algorithm," in Proceedings of the International Conference on Genetic and Evolutionary Methods (GEM), The Steering Committee of the World Congress in Computer Science, Computer …, 2013.
[38] M. Sababha, M. Zohdy, and M. Kafafy, "The enhanced firefly algorithm based on modified exploitation and exploration mechanism," Electronics, vol. 7, no. 8, pp. 132, 2018.
[39] M. Korpaas, A.T. Holen, and R. Hildrum, "Operation and sizing of energy storage for wind power plants in a market system," International Journal of Electrical Power & Energy Systems, vol. 25, no. 8, pp. 599–606, 2003.
[40] Y. Azoumah, D. Yamegueu, P. Ginies, Y. Coulibaly, and P. Girard, "Sustainable electricity generation for rural and peri-urban populations of sub-Saharan Africa: The 'flexy-energy' concept," Energy Policy, vol. 39, no. 1, pp. 131–141, 2011.
[41] A. Yadav, R. Bareth, M. Kochar, M. Pazoki, and R.A.E. Sehiemy, "Gaussian process regression-based load forecasting model," IET Generation, Transmission & Distribution, vol. 18, no. 5, pp. 899–910, 2024.
[42] Y. Ma, S. Wang, G. Liu, G. Tian, J. Zhang, and R. Liu, "State-of-charge balancing strategy of battery energy storage units with a voltage balance function for a bipolar DC microgrid," Applied Energy, vol. 356, pp. 122367, 2024.
[43] H. Elsaraf, M. Jamil, and B. Pandey, "Techno-economic design of a combined heat and power microgrid for a remote community in Newfoundland Canada," IEEE Access, vol. 9, pp. 91548–91563, 2021.
[44] S. Chakraborty, G. Modi, and B. Singh, "A cost optimized-reliable-resilient-realtime-rule-based energy management scheme for a SPV-BES-based microgrid for smart building applications," IEEE Transactions on Smart Grid, vol. 14, no. 4, pp. 2572–2581, 2022.
[45] A. Chakraborty and S. Ray, "Multi-objective operational cost management with minimum net emission of a smart microgrid," Electric Power Components and Systems, vol. 52, no. 10, pp. 1870–1891, 2024.
[46] A.A. Ellaboudy, "Saudi Electricity Company," Jan. 10, 2023 [cited 2024 Jan. 30]. Available from: https://www.climatescorecard.org/2023/01/saudi-electricity-company/.
[47] W.E. Office, "How wind can help us breathe easier," Aug. 24, 2023 [cited June 15, 2024]. Available from: https://www.energy.gov/eere/wind/articles/how-wind-can-help-us-breathe-easier#:~:text=CO_2%20Emissions%20from%20Different%20Energy%20Sources&text=Wind%20energy%20produces%20around%2011,2%2FkWh%20for%20natural%20gas.
[48] E.A. Alsema, Environmental Life Cycle Assessment of Solar Home Systems, Department of Science Technology and Society, Utrecht University Utrecht, 2000.
[49] E. Friedrich, S. Pillay, and C. Buckley, "Carbon footprint analysis for increasing water supply and sanitation in South Africa: A case study," Journal of Cleaner Production, vol. 17, no. 1, pp. 1–12, 2009.
[50] A.Q. Jakhrani, A.R.H. Rigit, A.K. Othman, S.R. Samo, and S.A. Kamboh, "Estimation of carbon footprints from diesel generator emissions," in Proceedings of the 2012 International Conference on Green and Ubiquitous Technology, IEEE, pp. 78–81, 2012.
[51] Z. Belboul, B. Toual, A. Kouzou, L. Mokrani, A. Bensalem, R. Kennel, and M. Abdelrahem, "Multiobjective optimization of a hybrid PV/Wind/Battery/Diesel generator system integrated in microgrid: A case study in Djelfa, Algeria," Energies, vol. 15, no. 10, pp. 3579, 2022.
[52] F.S. Kebede, J.C. Olivier, S. Bourguet, and M. Machmoum, "Reliability evaluation of renewable power systems through distribution network power outage modeling," Energies, vol. 14, no. 11, pp. 3225, 2021.
[53] S. Fang, T. Zhao, Y. Xu, and T. Lu, "Coordinated chance-constrained optimization of multi-energy microgrid system for balancing operation efficiency and quality-of-service," Journal of Modern Power Systems and Clean Energy, vol. 8, no. 5, pp. 853–862, 2020.
[54] R. Harvey, Z. Qu, and T. Namerikawa, "An optimized input/output-constrained control design with application to microgrid operation," IEEE Control Systems Letters, vol. 4, no. 2, pp. 367–372, 2019.
[55] K. Mongird, V. Viswanathan, P. Balducci, J. Alam, V. Fotedar, V. Koritarov, and B. Hadjerioua, "An evaluation of energy storage cost and performance characteristics," Energies, vol. 13, no. 13, pp. 3307, 2020.
[56] T.C. Accelerator, "Michigan Commercial & Industrial WIND Market Assets, Gaps & Recommendations EGLE Michigan Clean Energy Assets Roadmap Program," July 11, 2022 [cited 2024 July 11]. Available from: https://www.michigan.gov/egle/-/media/Project/Websites/egle/Documents/Programs/MMD/Energy/renewables/CA-CI-WIND-Roadmap-Report-FINAL3-102722.pdf?rev=0d77b7778d494ebcb44ec5a0bafc31e8.
[57] S. Reviews, "Solar panel cost Michigan," 2024 [cited 2024 July 1]. Available from: https://www.solarreviews.com/solar-panel-cost/michigan#:~:text=Levelized%20cost%20of%20power%20from,)%20is%2026.9%20cents%2FkWh.
[58] J. Wang, New Technologies and Business Models, 2024.
[59] W.E.T. Office, "Stakeholder Meeting 6: Combined Heat & Power," 2021 [cited June 10, 2024]. Available from: https://www.michigan.gov/-/media/Project/Websites/mpsc/workgroups/emerging-tech/MPGNewTech_Mtg_6_-_CHP_SlideDeck.pdf?rev=98e24e049941490d8f574ec91034cddb.
[60] R.P. Team, "The Life Expectancy of Your Diesel Generator," Aug. 21, 2020 [cited June 21, 2024]. Available from: https://www.reactpower.com/blog/the-life-expectancy-of-your-diesel-generator/.
[61] A. AlKassem, A. Draou, A. Alamri, and H. Alharbi, "Design analysis of an optimal microgrid system for the integration of renewable energy sources at a university campus," Sustainability, vol. 14, no. 7, pp. 4175, 2022.
[62] M.D. Qandil, R.S. Amano, and A.I. Abbas, "A stand-alone hybrid photovoltaic, fuel cell and battery system," in Proceedings of the Energy Sustainability Conference, American Society of Mechanical Engineers, 2018. A. AlKassem, A. Draou, A. Alamri, and H. Alharbi, "Design analysis of an optimal microgrid system for the integration of renewable energy sources at a university campus," Sustainability, vol. 14, no. 7, pp. 4175, 2022.

[63] J. Cotrell and W. Pratt, “Modeling the feasibility of using fuel cells and hydrogen internal combustion engines in remote renewable energy systems,” National Renewable Energy Lab. (NREL), Golden, CO, USA, 2003.